Proceedings of the IISE Annual Conference & Expo 2022
K. Ellis, W. Ferrell, J. Knapp, eds.

Optimal Speed-based Cost of Resilience in Electrified High-speed Railway Systems

Weijie Pan, Ekundayo Shittu

The George Washington University, Washington, D.C, USA

Abstract

There is no doubt that there is an increase in the penetration of electrical energy into the operation of high-speed railway systems (HSR). This is even more pronounced with the increasing trends in smart electric multiple units (EMU). The operational speed serves as a metric for punctuality and safety, as well as a critical element to maintain the balance between energy supply and consumption. The speed-based regenerative energy from EMU's braking mode could be utilized in the restoration of system operation in the aftermath of a failure. This paper optimizes the system resiliency with respect to the operational speed for the purpose of restoration by minimizing the total cost of implementing recovery measures. By simultaneously valuating the dual-impact of any given fault on the speed deterioration level from the railway operation systems (ROS) side and the power supply and demand unbalance level from the railway power systems (RPS) side, this process develops an adaptive two-dimension risk assessment scheme for prioritizing the handling of different operational zones that are cascaded in the system. With the aid of an integrated speed-based resilience cost model, we determine the optimal resilience time, speed modification plan, and energy allocation strategy. The outcome from implementing this routine in a real-world HSR offers a pioneering decision-making strategy and perspective on optimizing the resilience of an integrated system.

Keywords: System Resilience, Regenerative Energy, Risk Assessment, High-Speed Railway Systems

Nomenclature

HSR	High-speed railway systems	ε_j	Speed deterioration rate at the fault zone j
EMU	Electric multiple units	D_i	Geographic distance of the operational zone i (km)
ROS	Railway operation systems	L_i	Geographic length of the operational zone i (km)
RPS	Railway power systems	n_i	Train number under operation inside operational zone i
F	Set of fault zones	f_{trc-i}	Tractive force within the operational zone i (kN)
i	Index number of the operational zone	S_i	Speed variance level at the operational zone i
j	Index number of fault zone	E_i	Power unbalance level at the operational zone i
N	Total number of operational zones	W_i	Risk weight coefficient at the operational zone i
V	Voltage on traction overhead line (kV)	I_{max}	The maximum current on traction overhead line (A)

v_{ini-i} v_{det-i} v_{opt-i}	Initial speed / deteriorated speed / optimal speed within the operational zone i (km/h)
P_{ini-i} P_{trc-i} P_{opt-i}	Initial / tractive / optimal power demand at the operational zone i (kWh)
G_{ini-i} G_{loss-i}	Initial / lost power generation at the operational zone i (kWh)
$PT_{(i,i+1)}$	Regenerative power transferred from operational zone i to operational zone $(i+1)$ (kWh)
∇T_i	Optimal system resilience time at the operational zone i (min)

1. Introduction

The development and construction of high-speed railway systems (HSR) bring great convenience and improvements to inter-city transportation. Communities across the world rely on HSR every day for transportation. From the system structure perspective, the modern electrified HSR is a highly integrated system consisting of a railway operation system (ROS) and a railway power system (RPS) [1]. The ROS mainly supplies power to the electric multiple units (EMU) while the RPS mainly transmits power from power plants to zonal traction substations. However, the entire system is fully exposed to the natural environment thereby increasing the risk of being vulnerable to contingencies, such as harsh lightning and snowstorms [2].

As a public transportation option, the top priority of HSR is operational safety and punctuality. A dilemma is that maintaining a faster speed usually poses a higher risk to operational safety, such that in the event of emergencies and

system faults, it is challenging for a railway company to instantaneously realize a trade-off between safety and operation efficiency. Additionally, the energy demand from EMU's operation is a huge portion of engineering expenses [3]. If the system is forced to stay in a stagnant state under the circumstance of any unanticipated system fault, the financial loss from the power supply and demand unbalance is another immeasurable sunk cost. Power system resiliency greatly depends on the flexibility of power transmission and the rapidity of energy generation recovery [4]. The resilience time is usually treated as a pivotal element in evaluating the system resilience, but it greatly depends on the operational speed of HSR. The objective of this paper is to improve system resilience by controlling EMU's operational speed while the power balance is being simultaneously maintained.

2. Literature Review

Numerous studies have analyzed the electrified HSR structure and characteristics. For example, a holistic modeling method for evaluating the power supply capability for DC railway traction power systems was developed by integrating the train kinematics, driving controls, power supply infrastructure, and multiple fault modes [5]. In related work, [6] proposed a DC power network modeling method including train motion and power network simulation to evaluate the energy consumption in RPS. The simulation results illustrate the feasibility of using regenerative energy control to improve energy utilization efficiency under different operational modes. A qualitative approach has been proposed for the development of railway electrified smart grids with a focus on the contribution from the regenerative braking mode through the spatial and temporal shifting of power consumption between neighboring electrical grids [1]. This approach also considers a price-oriented driving mode based on the realization of the power transfer function to minimize the operational cost. Additionally, [7] presented the effectiveness of connecting distributed generations to HSR for power quality improvement purposes. Nevertheless, there is a research gap in linking operational speed management with HSR resilience improvement.

System resiliency is an equally important concept and is under intense discussions [8]. For instance, [9] and [10] present a comprehensive review of the existing approaches for system self-healing purposes and provide a promising policy framework to incentivize the investment into electricity network resilience. [11] discusses the applicability of a multicriteria decision analysis method (MCDA) under various fault circumstances. [12] and [13] present a detailed category of fault types and their origins in power systems. [14] proposes an improved analytical network process (ANP) to evaluate the relative importance of each risk evaluation index. [15] proposes a holistic model regarding the total cost involved in the power system resilience period by conducting system re-configuration. However, the risk management and resilience study have not been fully applied to HSR with treating the speed as a decision factor.

Combining all those issues, including regenerative energy utilizations, risk assessment methods, system resilience control models, and system operational cost considerations, this work presents a holistic methodology to apply those topics to electrified HSR systems.

3. Methodology

The risk evaluation is a necessary step to obtain a better understanding of the cascading impact on the whole system from an unexpected system fault [16]. This research evaluates the dual impact risk of the system fault on both ROS and RPS sides, including a speed deterioration assumption and a two-dimensional risk assessment matrix method. With the outcomes from the proposed risk evaluation methodology, an optimal speed-based resilience cost model is derived to offer the ultimate decision of variables to safeguard system operations and minimize the financial cost arising from the energy generation compensation and potential energy demand variance.

3.1. **Speed Deterioration Assumption**

In this work, a zonal speed deterioration assumption is presented as the worst outcome of the cascading impact from an uncertain fault location. The proposed assumption is inspired by Fitts's law that describes a movement relationship between time and distance [17]: the time required to rapidly move a point to a target is a function of the distance to the target and the width of the target. It takes a longer time to reach the central point of the target if the distance is longer, while it takes a shorter time if the size of the target is larger. For the speed deterioration assumption in this work. If the distance between any operational zone and the fault zone is longer, the impact on its speed allocation is smaller. Equation (1) below displays the quantified speed deterioration assumption.

$$v_{det-i} = v_{ini-i} \times \left(1 - \varepsilon_j \times \left(1 - log_2^{\left(\frac{|D_i - D_j|}{D_N - D_1} + 1\right)}\right)\right) \qquad (j \in F) \tag{1}$$

In this work, we assume the worst case of the system deterioration is for trains to keep a minimum operational speed

within the fault zone. The minimum operational speed can safeguard system from turning into a complete stagnant state, which would greatly impact the punctuality. Equation (2) defines the speed deterioration rate.

$$\varepsilon_j = \frac{v_j - v_{min}}{v_j} \qquad (\ j \in F\ ) \tag{2}$$

3.2. **Two-Dimensional Risk Assessment Matrix**

When an unexpected fault happens to HSR, no matter which subsystem it happens in, both ROS and RPS subsystem will be impacted. This paper proposes a two-dimensional risk assessment method to evaluate the dual impact from a single fault. For RPS side, the risk index is the unbalance level between power supply and demand. For ROS side, the risk index is the speed variance level, which directly impacts the punctuality. The flow chart in **Figure 1** presents the steps of conducting the proposed two-dimensional risk assessment procedure.

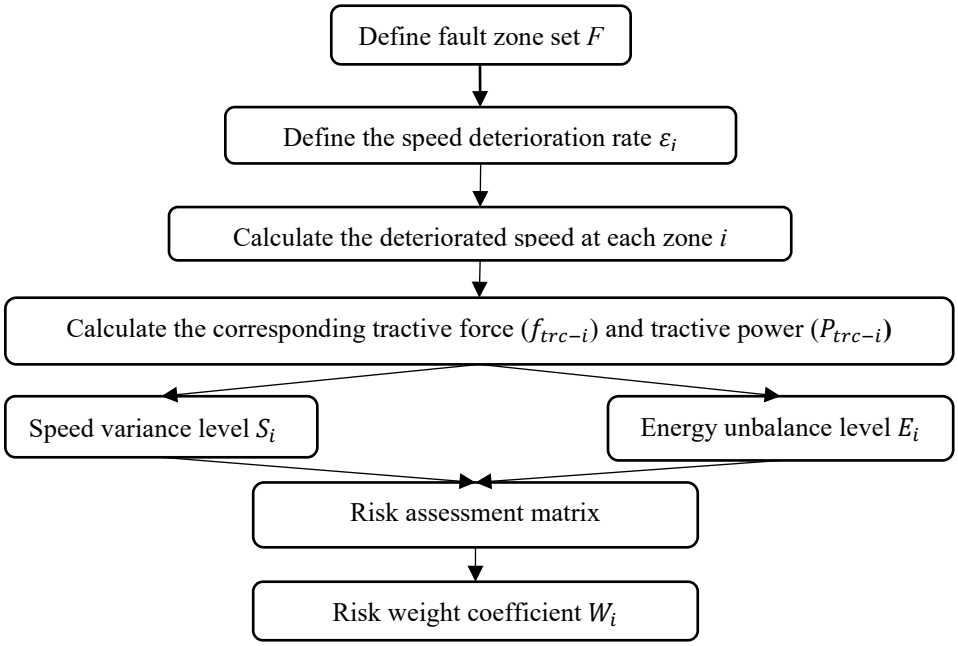

Figure 1: Flow chart of conducting two-dimensional risk assessment model.

The underlying modeling framework is described by the following equations.

$$f_{trc-i} = a \times v_i^2 + \mathrm{b} \times v_i + c \tag{3}$$

$$P_{trc-i} = f_{trc-i} \times v_i \times n_i \tag{4}$$

$$S_i = 1 + \frac{|V_{ini-i} - V_{act-i}|}{V_{ini-i}} \tag{5}$$

$$E_i = 1 + \frac{|G_{ini-i} - G_{act-i}|}{P_{ini-i}} \tag{6}$$

$$\text{Risk Matrix} = \begin{bmatrix} S_1 & E_1 \\ \vdots & \vdots \\ S_N & E_N \end{bmatrix} \tag{7}$$

$$W_i = \frac{\sqrt{(S_i - 1)^2 + (E_i - 1)^2}}{\sum_{i=1}^{N} \sqrt{(S_i - 1)^2 + (E_i - 1)^2}} \tag{8}$$

Equation (3) describes the relationship between the tractive force and the speed, where a, b, c is the technical constant [6]. Equation (4) presents the calculation formula of tractive power energy. Equation (5) and Equation (6) show the quantitative definition of speed variable level and power unbalance level, respectively. Equation (7) and Equation (8) represent the form of risk assessment matrix and risk weight calculation, respectively.

3.3. **Speed-based Cost of Resilience Model**

When the severity level for each operational zone is defined, the optimal operation management strategy is proposed to minimize the total cost for system resilience purpose. In this paper, the inverse power flow from the regenerative braking mode within the neighboring operational zones is used as an energy compensation strategy for the fault location where the power generation is lost. **Figure 2** below shows a conceptual presentation of the utilization of regenerative energy under system resilience period.

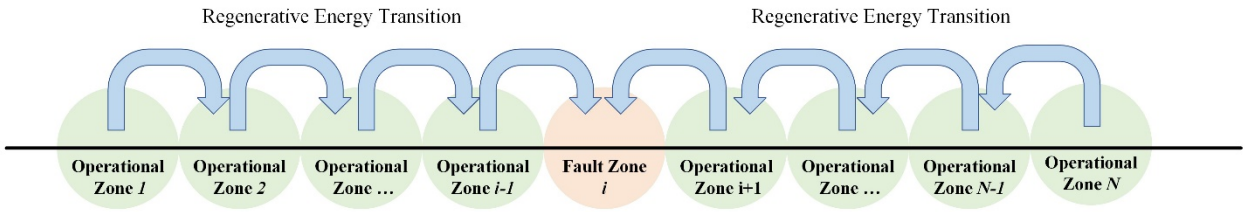

Figure 2: Power transition from regenerative braking mode.

The objective function is presented in Equation (9), where C is the unit cost for power generation. The constrains are described in the following equations set. Equation (10) and Equation (11) present the calculation of tractive force and tractive power demand, respectively. Equation (12) describes the ideal power balance relationship between generation and demand. Equation (13) and Equation (14) describe the selection of optimal resilience time of the system and the calculation of resilience time within each fault zone, respectively. Equation (15) to Equation (19) define the regenerative power transmitted from the neighboring operational zones into the fault zone with the transmission limitation being considered. Equation (20) to Equation (23) define the optimal inverse power flow of regenerative energy among the rest of operational zones with the transmission limitation being considered.

$$\min_{v_{trc-i} \le v_i \le v_{ini-i}} OF(v_i) = \sum_{i \in F} G_{loss-i}(v_i) \times \nabla T(v_i) \times C + \sum_{i}^{N} W_i \times \left| P_{opt-i}(v_i) - P_{ini-i} \right| \times \nabla T(v_i) \times C \quad (9)$$

$s.to.$

$$P_{opt-i}(v_i) = v_i \times f_{trc-i}(v_i) \times n_i \quad (10)$$

$$f_{trc-i}(v_i) = a \times v_i^2 + \mathrm{b} \times v_i + c \quad (11)$$

$$G_{loss-i}(v_i) = P_{opt-i}(v_i) \quad i \in F \quad (12)$$

$$\nabla T(v_i) = \min\{\nabla T_i(v_i)\} \quad i \in F \quad (13)$$

$$\nabla T_i(v_i) = \frac{L_i}{v_i} \quad i \in F \quad (14)$$

$$PT_{(i-1,i)} + PT_{(i+1,i)} \ge P_{opt-i}(v_i) \quad i \in F \quad (15)$$

$$PT_{(i-1,i)} = P_{opt-(i-1)}(v_{i-1}) \quad i \in F \quad (16)$$

$$\frac{PT_{(i-1,i)}}{n_{i-1}} \le V \times I_{max} \quad i \in F \quad (17)$$

$$PT_{(i+1,i)} = P_{opt-(i+1)}(v_{i+1}) \quad i \in F \quad (18)$$

$$\frac{PT_{(i+1,i)}}{n_{i+1}} \le V \times I_{max} \quad i \in F \quad (19)$$

$$PT_{(i,i+1)} = P_{opt-i}(v_i) \quad i \notin F \text{ and } i < j \quad (20)$$

$$\frac{PT_{(i,i+1)}}{n_i} \le V \times I_{max} \quad i \notin F \text{ and } i < j \quad (21)$$

$$PT_{(i,i-1)} = P_{opt-i}(v_i) \quad i \notin F \text{ and } i > j \quad (22)$$

$$\frac{PT_{(i,i-1)}}{n_i} \le V \times I_{max} \quad i \notin F \text{ and } i > j \quad (23)$$

3.4. **Data and Modeling Platform**

In this work, the Beijing-Shanghai high-speed railway system [18] is used for verification. The whole length of this train line is 1302 km with 23 main destination stations (22 operational zones). The standard operational speed of bullet trains on this train line is 350km/h with a minimum operational speed of 200km/h, the standard length of a 4M4T EMU is 200 meters, with a fixed headway time of 5 minutes. The corresponding technical constant a, b, c is 0.0035, -2.2, 450 respectively. The **Table 1** below displays the basic system parameters.

Table 1: System parameters of Beijing-Shanghai high-speed railway system

$Zone_i$	1	2	3	4	5	6	7	8
D_i (L_i)	59 (59)	131 (72)	219 (88)	327 (108)	419 (92)	462 (43)	533 (71)	589 (56)
v_{ini-i} (n_i)	330 (2)	335 (2)	340 (3)	350 (3)	345 (3)	310 (1)	335 (2)	330 (2)
$Zone_i$	**9**	**10**	**11**	**12**	**13**	**14**	**15**	**16**
D_i (L_i)	625 (36)	688 (63)	767 (79)	844 (77)	897 (53)	959 (62)	1018 (59)	1087 (69)
v_{ini-i} (n_i)	300 (1)	330 (2)	340 (2)	340 (2)	330 (1)	330 (2)	330 (2)	335 (2)
$Zone_i$	**17**	**18**	**19**	**20**	**21**	**22**		
D_i (L_i)	1112 (25)	1144 (32)	1201 (57)	1227 (26)	1259 (32)	1302 (43)		
v_{ini-i} (n_i)	280 (1)	290 (1)	330 (2)	280 (1)	290 (1)	310 (1)		

The risk assessment model is conducted on MATLAB, and the optimization algorithm is conducted on GAMS with DNLP solver. The unit cost for power generation is assumed as $1.00 per kWh.

4. Results

Figure 3 below displays the risk weight dispersion from the risk assessment model with a single system fault at each operational zone. **Figure 4** below shows the optimal resilience time and minimum resilience cost in the event of a single system fault at each operational zone, corresponding to the risk assessment cases.

The simulation result in **Figure 3** shows that a greater weight variance is indicative of a more dispersive weight distribution, and vice versa. A more dispersive weight distribution more likely occurs when the fault happens at the endpoint operational zones of the system line. A more concentrative risk distribution implies a more even speed and power allocation strategy needs to be applied to the rest of the operational zones besides the fault zone.

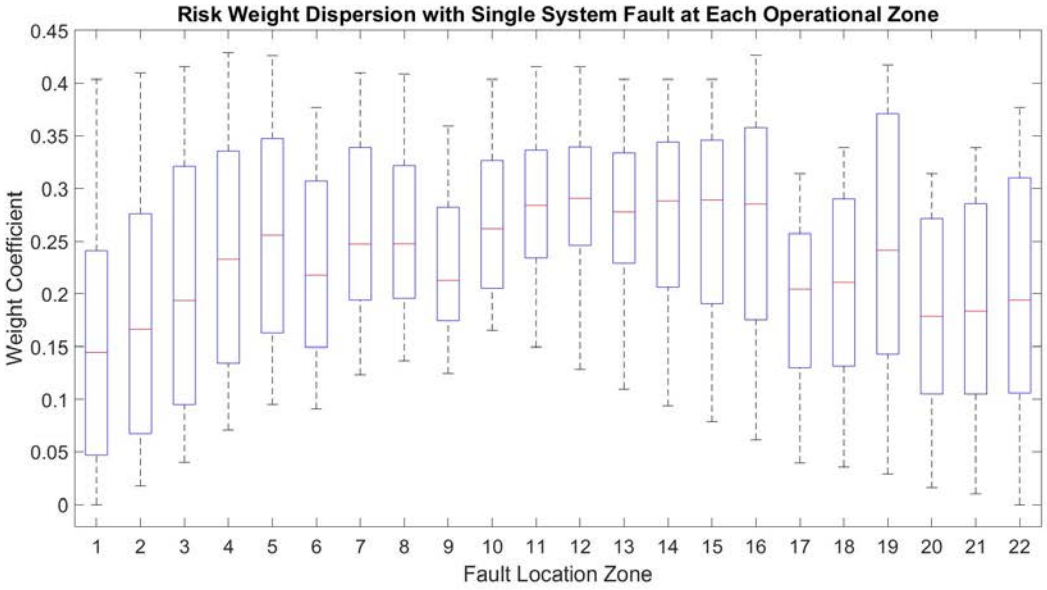

Figure 3: Risk weight dispersion with single fault at each operational zone

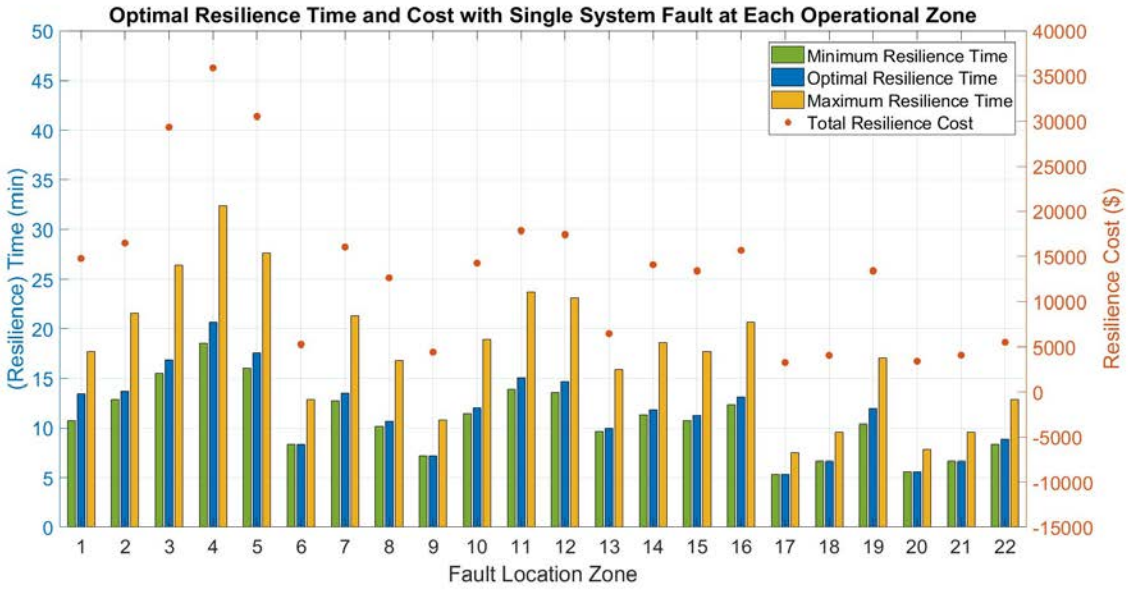

Figure 4: Optimal resilience time and cost with single system fault at each operational zone

The result in **Figure 4** shows that optimal resilience time is shorter than the one under the worst operational speed case (deteriorated speed case) and slightly longer than the one with scheduled operational speed (the case without any system faults). This result generally implies that trains have to be evacuated from the fault zone as quickly as

possible. However, the speed cannot exceed the initial scheduled speed due to the constrains of schedule timetable and the final cost of the unexpected extra energy consumption above the scheduled power consumption.

5. Conclusions

This study treats the speed-based regenerative power of HSR as a pivotal element to realize the system resilience purpose. The derived optimal resilience time offers the system operational decision maker with a rational evaluation of resilience measures while keeping the system under an acceptable operational status instead of a total stagnation. This research also implements a two-dimensional risk assessment method to determine the risk distribution situation of an integrated system with a long-distance connection characteristic. The result shows that a more concentrative risk distribution occurs if an unexpected system fault happens around the midpoint location of the system. The risk weight derived from the risk assessment model is used to determine the priority level of modifying energy unbalance in the event of realizing the system resilience. The proposed optimization model combines a varying load performance, energy balance and financial considerations simultaneously. The successful validation of the proposed methodology sheds a light on the possibility of realizing the resilience purpose of an integrated system by utilizing the performance characteristics of varying load. The research outcomes can be expanded to a more complicated hybrid system where multiple types of energy consumers are interconnected for a complementary energy coordination purpose in the event of contingencies.

References

[1] E. Pilo de la Fuente, S. K. Mazumder and I. G. Franco, "Railway Electrical Smart Grids: An introduction to next-generation railway power systems and their operation.," *in IEEE Electrification Magazine*, vol. 2, no. 3, pp. 49-55, Sept. 2014, doi: 10.1109/MELE.2014.2338411.

[2] R. A. Munteanu, A. Cretu, D. Iudean, A. Ceclan and D. D. Micu, "Reliability Evaluation of Modern Railway Systems," *the 12th Mediterranean Conference on Power Generation*, *Transmission, Distribution and Energy Conversion (MEDPOWER 2020)*, 2020, pp. 202-207, doi: 10.1049/icp.2021.1286.

[3] S. Kaewunruen, J. Sresakoolchai, and J. Peng, "Life Cycle Cost, Energy and Carbon Assessments of Beijing-Shanghai High-Speed Railway," *Sustainability*, vol. 12, no. 1, pp. 206, Dec. 2019.

[4] W. Li, *Risk Assessment of Power Systems: Models, Methods, and Applications,* Wiley-IEEE Press, 2014.

[5] Z. Tian, N. Zhao, S. Hillmansen, S. Su, and C. Wen, "Traction Power Substation Load Analysis with Various Train Operating Styles and Substation Fault Modes," *Energies*, vol. 13, no. 11, pp. 2788, Jun. 2020.

[6] Z. Tian, S. Hillmansen, C. Roberts, P. Weston, N. Zhao, L. Chen, Mingwu. Chen, "Energy evaluation of the power network of a DC railway system with regenerating trains," *IET Electrical Systems in Transportation*, vol. 6, no. 2, pp. 41–49, Jun, 2016.

[7] W. Pan, S. C. Dhulipala, and A. S. Bretas, "DG Integration and Power Quality Management in Railway Power Systems: A Distributed Approach," in *10th Bulk Power Systems Dynamics and Control Symposium, 2017, Espinho, Portugal*, pp. 1–7, IEEE, 2017.

[8] M. Panteli and P. Mancarella, "The Grid: Stronger, Bigger, Smarter ? : Presenting a Conceptual Framework of Power System Resilience," *in IEEE Power and Energy Magazine*, vol. 13, no. 3, pp. 58-66, May-June 2015, doi: 10.1109/MPE.2015.2397334.

[9] E. Shittu, A. Tibrewala, S. Kalla, and X. Wang, "Meta-analysis of the strategies for self-healing and resilience in power systems," *Adv. Appl. Energy*, vol. 4, p. 100036, Nov. 2021, doi: 10.1016/j.adapen.2021.100036.

[10] E. Shittu and J. R. Santos, "Electricity Markets and Power Supply Resilience: an Incisive Review," Curr. Sustain. Energy Rep., vol. 8, no. 4, pp. 189–198, Dec. 2021, doi: 10.1007/s40518-021-00194-4.

[11] J. M. Keisler and I. Linkov. "Use and Misuse of MCDA to Support Decision Making Informed by Risk". *Risk Analysis.2020 Sep*, vol. 41, no. 9, pp.1513-1521, Nov.2020, doi: 10.1111/risa.13631.

[12] U. G. Knight, *Power Systems in Emergencies: From Contingency Planning to Crisis Management,* Wiley, 2001.

[13] A. Mar, P. Pereira, and J. F. Martins, "A Survey on Power Grid Faults and Their Origins: A Contribution to Improving Power Grid Resilience," *Energies*, vol. 12, no. 24, pp. 4667, Dec. 2019.

[14] L.Cheng, Y,Wang and Y. Peng, "Research on risk assessment of high-speed railway operation based on network ANP," *Smart and Resilient Transportation*, vol. 3, no. 1, pp.37-51, May. 2021, doi:10.1108/SRT-10-2020-0024.

[15] M. Ghiasi et al., "Resiliency/Cost-Based Optimal Design of Distribution Network to Maintain Power System Stability Against Physical Attacks: A Practical Study Case," *in IEEE Access*, vol. 9, pp. 43862-43875, 2021, doi: 10.1109/ACCESS.2021.3066419.

[16] I. Deluque, E. Shittu, and J. Deason, "Evaluating the reliability of efficient energy technology portfolios," *EURO J. Decis. Process.*, vol. 6, no. 1, pp. 115–138, Jun. 2018, doi: 10.1007/s40070-018-0077-4.

[17] "Fitts's Law", Wikipedia, [Online], Available: https://en.wikipedia.org/wiki/Fitts%27s_law.

[18] "Beijing-Shanghai High-speed Railway", Wikipedia, [Online], Available: https://en.wikipedia.org/wiki/Beijing%E2%80%93Shanghai_high-speed_railway.